

## Supplementary materials

A prospective study of the protective effect of SARS-CoV-2-specific antibodies and T cells in Moscow residents

Ivan A. Molodtsov<sup>1,\*</sup>, Evgenii Kegeles<sup>2,\*</sup>, Alexander N. Mitin<sup>3,\*</sup>, Olga Mityaeva<sup>2,\*</sup>, Oksana E. Musatova<sup>4,\*</sup>, Anna E. Panova<sup>5,\*</sup>, Mikhail V. Pashenkov<sup>3,\*</sup>, Iuliia O. Peshkova<sup>6,\*</sup>, Alsalloum Almaqdad<sup>2</sup>, Walaa Asaad<sup>2</sup>, Anna S. Budikhina<sup>3</sup>, Aleksander S. Deryabin<sup>4</sup>, Inna V. Dolzhikova<sup>7</sup>, Ioanna N. Filimonova<sup>4</sup>, Alexandra N. Gracheva<sup>5</sup>, Oxana I. Ivanova<sup>1,8</sup>, Anastasia Kizilova<sup>2</sup>, Viktoria V. Komogorova<sup>3</sup>, Anastasia Komova<sup>2,9</sup>, Natalia I. Kompantseva<sup>5</sup>, Denis A. Lagutkin<sup>5</sup>, Yakov A. Lomakin<sup>4</sup>, Alexandra V. Maleeva<sup>6</sup>, Elena V. Maryukhnich<sup>1,8</sup>, Afraa Mohammad<sup>2</sup>, Vladimir V. Murugin<sup>3</sup>, Nina E. Murugina<sup>3</sup>, Anna Navoikova<sup>2</sup>, Margarita F. Nikonova<sup>3</sup>, Leyla A. Ovchinnikova<sup>4</sup>, Natalia V. Pinegina<sup>1,8</sup>, Daria M. Potashnikova<sup>1,8</sup>, Elizaveta V. Romanova<sup>1</sup>, Aleena A. Saidova<sup>1</sup>, Nawar Sakr<sup>2</sup>, Anastasia G. Samoilo<sup>5</sup>, Yana Serdyuk<sup>6</sup>, Naina T. Shakirova<sup>6</sup>, Nina I. Sharova<sup>3</sup>, Savely A. Sheetikov<sup>6</sup>, Anastasia F. Shemetova<sup>5</sup>, Liudmila Shevkova<sup>2,9</sup>, Alexander V. Shpektor<sup>8</sup>, Anna Trufanova<sup>2</sup>, Anna V. Tvorogova<sup>1</sup>, Valeria M. Ukrainskaya<sup>4</sup>, Anatoliy S. Vinokurov<sup>5</sup>, Daria A. Vorobyeva<sup>1,8</sup>, Ksenia V. Zornikova<sup>6</sup>, Grigory A. Efimov<sup>6,†</sup>, Musa R. Khaitov<sup>3,†</sup>, Ilya A. Kofiadi<sup>3,†</sup>, Alexey A. Komissarov<sup>1,†</sup>, Denis Y. Logunov<sup>7,†</sup>, Nelli B. Naigovzina<sup>8,†</sup>, Yury P. Rubtsov<sup>4,†</sup>, Irina A. Vasilyeva<sup>5,†</sup>, Pavel Volchkov<sup>2,9,†,#</sup>, and Elena Vasilieva<sup>1,8,†</sup>

<sup>1</sup> Clinical City Hospital named after I.V. Davydovsky, Moscow Department of Healthcare, 109240, 11/6 Yauzskaya str., Moscow, Russia

<sup>2</sup> Genome Engineering lab, Moscow Institute of Physics and Technology, 141700, 9  
Institutskiy per., Dolgoprudniy, Russia

<sup>3</sup> National Research Center – Institute of Immunology Federal Medical-Biological Agency of  
Russia, 115522, 24 Kashirskoye shosse, Moscow, Russia

<sup>4</sup> Shemyakin-Ovchinnikov Institute of Bioorganic Chemistry of the Russian Academy of  
Sciences, 117997, 16/10 Miklukho-Maklaya str., Moscow, Russia

<sup>5</sup> National Medical Research Center for Phthisiopulmonology and Infectious Diseases of the  
Ministry of Health of the Russian Federation, 127473, 4 Dostoevsky str., Moscow, Russia

<sup>6</sup> National Research Center for Hematology, 125167, 4a Novozykovskii proezd, Moscow,  
Russia

<sup>7</sup> Federal State Budget Institution "National Research Centre for Epidemiology and  
Microbiology named after Honorary Academician N F Gamaleya" of the Ministry of Health  
of the Russian Federation, 123098, 18 Gamaleya str., Moscow, Russia

<sup>8</sup> A.I. Yevdokimov Moscow State University of Medicine and Dentistry, 127473, 20  
Delegatskaya str., Moscow, Russia

<sup>9</sup> Research Institute of Personalized Medicine, National Center for Personalized Medicine of  
Endocrine Diseases, The National Medical Research Center for Endocrinology, 117036, 11  
Dmitry Ulyanov str., Moscow, Russia

\* These authors contributed equally to this work as co-first authors

† These authors contributed equally to this work as co-senior authors

# Corresponding author: vpwww@gmail.com (P.V.)

### *Supplementary Section 1: Positivity Criteria*

For ELISPOT and flow cytometry tests, no pre-defined positivity criteria existed. In order to create positivity criteria which would optimally discriminate between people who were diagnosed with COVID-19 and those who had not been so diagnosed (in a manner similar to antibody test positivity criteria), we first selected two groups of patients. The first group, or ‘negative group,’ consisted of patients with no earlier COVID-19 or COVID-19 contacts reported by state authorities, no self-reported COVID-19 or COVID-19 contacts, no ARI symptoms six months prior to the inclusion reported, with IgG, Mindray < 1 AU/mL, and with IgM, Mindray < 1 COI. The second group, or ‘positive group’, consisted of the patients with PCR-confirmed COVID-19 who recovered before the study, as reported by state authority, and self-reported COVID-19.

There were a total of 401 patients in the negative group, out of whom 209 had ELISpot results and 292 had flow cytometry results, and there were 563 patients in the positive group, out of whom 303 had ELISpot results and 318 had flow cytometry results.

We then developed the criteria which would allow us to reach the optimal separation between two such groups using results of ELISpot or flow cytometry tests. Such a criterion has an idea behind it of labeling patients who were earlier ill with COVID-19 as positive and those who were not as negative, in the same sense as positivity criteria for serology test developed by the manufacturer. The major limitation of this method arises from our inability to rule out earlier infection with SARS-Cov-2 by any other means except by using IgG levels.

#### *ELISpot Positivity Criteria*

For each ELISpot measurement, there are four main values provided in this study: number of spots (NoS) for M protein, NoS for N protein, NoS for S protein, and NoS for negative control. To build positivity criteria for each of the proteins, NoS for this protein and for negative control were used.

The commonly used positivity criteria in ELISpot are based on comparison of negative control with experiment and selecting some additive and multiplicative boundary relations between these two values. Such a method, however, is based on an underlying hypothesis that a value observed in a negative control is not a random value but rather results from some underlying sample characteristic which may affect both non-control and negative control

values. In order to check this hypothesis and select the optimal positivity criteria, the following testing procedure was used.

We supposed that there exists a two-parametric threshold which separates positive and negative groups of patients which can be expressed as  $\text{NoS}_{\{\text{protein}\}} = a \cdot \text{NoS}_{\{\text{negative\_control}\}} + b$ . We then selected a set of fixed 'a'  $\in \{0; 0.5; 1; 2\}$ , and for each 'a<sub>i</sub>' from this set we tested the all possible 'b' values to calculate the optimal false positive rate (FPR) and true positive rate (TPR) and build a ROC curve. For such a ROC curve, the area under the curve AUC<sub>i</sub> was calculated, and optimal 'b<sub>i</sub>' was selected (as 'b<sub>i</sub>' which minimizes Euclidian distance to (FPR=0, TPR=1) point,  $\text{FPR}^2 + (1 - \text{TPR})^2$ ). We then compared AUC<sub>i</sub> for different a<sub>i</sub> (see Supplementary Figure S1).

We found that, although for the N protein ROC AUC was maximized with a=0, for the M protein with a=0.5, and for the S protein with a=1, in all cases the differences between AUC for all 'a' values were minor. The resulting optimal TPR and FPR for each of the curves were nearly identical, and all models performed nearly identically. This arises from the fact that multiplication factor 'a' will come into play only for the larger values of NoS in the negative control, which are effectively absent from the dataset, and for smaller values only the additive part, 'b', is important. Thus, we decided to set 'a' equal to zero and to use positivity criteria which suppose independence of experimental values from negative control values. The optimal values of 'b' were 9, 4, and 13 for the M, N, and S proteins, respectively, meaning that samples with protein NoS above this threshold were labeled as positive, and samples with protein NoS below or equal to this threshold were labeled as negative for the corresponding protein.

For all proteins, the FPR fell in the range ~0.15–0.2, and optimal TPR fell in the range of ~0.8–0.9, which in a sense characterizes the ability of the positivity criteria to correctly distinguish patients who were earlier ill with COVID-19 from those who were not.

#### *Flow Cytometry Positivity Criteria*

For flow cytometry positivity criteria, an analysis similar to the ELISpot data one was used. Fractions of CD4<sup>+</sup> or CD8<sup>+</sup> T cells expressing IFN $\gamma$  only, IL2 only, or both cytokines out of the total number of CD4<sup>+</sup> or CD8<sup>+</sup> T cells, respectively, were calculated in experiment and negative control; we also additionally calculated fractions of all CD4<sup>+</sup>, CD8<sup>+</sup> cells expressing IFN $\gamma$  and all CD4<sup>+</sup>, CD8<sup>+</sup> cells expressing IL2. Thus, experimental value and negative

control were paired for each type of cell fractions and were used in the search for the optimal threshold of  $\text{Fraction}_{\{\text{experiment}\}} = a \cdot \text{Fraction}_{\{\text{negative\_control}\}} + b$  type for 'a' <out\_of> {0;0.5;1;2}.

However, there was a significant difference between the positivity analysis performed in ELISpot and that in the flow cytometry studies: since the study was multi-central and different devices were used, the positivity criteria were evaluated independently for each of the three study centers, labeled below as Center #1, #2 and #3.

Supplementary Table S1 contains information about the highest AUC achieved, and the corresponding 'a' value and optimal 'b' for this 'a' for each cell fraction and each center (see Supplementary Figure S2 for an example of analysis). The analysis of results allowed us to make the following conclusions:

- positivity criteria were different for different centers;
- in many cases, the maximum ROC AUC was achieved for non-zero 'a' and was higher than for ROC with  $a=0$  (data not provided; see Supplementary Figure S2 for an example in the case of the fraction of CD4<sup>+</sup> T cells expressing IFN $\gamma$  only);
- for Center #2, the maximum ROC AUC was achieved for  $a=0$ , which signifies the independence between negative control and experiment, while for Centers #1 and #3 the maximum ROC AUC was always achieved for non-zero  $a$ ;
- the ROC AUC for separation of two groups was the highest in Center #3, lower in Center #2, and lowest in Center #1 for all CD4<sup>+</sup> cell fractions;
- among different CD8<sup>+</sup> cell fractions, only the fraction of CD8<sup>+</sup> T cells expressing IFN $\gamma$  allowed us to distinguish between positive and negative groups, with AUC considerably lower if compared to CD4<sup>+</sup> cell fractions.

As a result of these observations, in contrast with ELISpot positivity criteria selection, we did not select  $a=0$  as a pre-set parameter but rather used optimal 'a' and 'b' resulting from the analysis. Criteria selected for each center and each cell fraction were afterwards used only for the data coming from this particular center. At the same time, it should be noted that for all cases ROC AUC for  $a=0$  was comparable or equal to ROC AUC for optimal 'a', which means that cell fractions can be used as a quantitative metric of T cell immune response without additional corrections by negative control.

Supplementary Table S1

Cell Fraction	Center	optimal a	optimal b	ROC AUC for optimal a
<b>CD4<sup>+</sup></b>				
Fraction of CD4 <sup>+</sup> IFN $\gamma$ <sup>+</sup> out of all CD4 <sup>+</sup>	Center # 1	1	1.7E-04	0.631
	Center # 2	0	4.9E-04	0.726
	Center # 3	1	1.7E-04	0.783
Fraction of CD4 <sup>+</sup> IL2 <sup>+</sup> out of all CD4 <sup>+</sup>	Center # 1	1	1.8E-04	0.677
	Center # 2	0	2.3E-04	0.732
	Center # 3	0.5	3.5E-04	0.854
Fraction of CD4 <sup>+</sup> IL2 <sup>+</sup> IFN $\gamma$ <sup>+</sup> out of all CD4 <sup>+</sup>	Center # 1	2	8.7E-05	0.721
	Center # 2	0	8.5E-05	0.732
	Center # 3	0.5	1.6E-04	0.915
Fraction of all CD4 <sup>+</sup> IFN $\gamma$ <sup>+</sup> out of all CD4 <sup>+</sup>	Center # 1	2	2.0E-04	0.649
	Center # 2	0	5.3E-04	0.740
	Center # 3	1	5.3E-04	0.848
Fraction of all CD4 <sup>+</sup> IL2 <sup>+</sup> out of all CD4 <sup>+</sup>	Center # 1	2	1.8E-04	0.704
	Center # 2	0	2.8E-04	0.745
	Center # 3	0.5	6.0E-04	0.881
Fraction of all activated CD4 <sup>+</sup>	Center # 1	1	8.1E-04	0.676
	Center # 2	0	6.7E-04	0.757
	Center # 3	0.5	8.5E-04	0.847
<b>CD8<sup>+</sup></b>				
Fraction of CD8 <sup>+</sup> IFN $\gamma$ <sup>+</sup> out of all CD8 <sup>+</sup>	Center # 1	2	-1.3E-03	0.581
	Center # 2	0	5.6E-04	0.689
	Center # 3	0.5	2.3E-04	0.648
Fraction of CD8 <sup>+</sup> IL2 <sup>+</sup> out of all CD8 <sup>+</sup>	Center # 1	2	1.5E-07	0.525
	Center # 2	0	3.2E-05	0.535
	Center # 3	2	-9.5E-05	0.546
Fraction of CD8 <sup>+</sup> IL2 <sup>+</sup> IFN $\gamma$ <sup>+</sup> out of all	Center # 1	2	0.0E+00	0.574

<b>CD8<sup>+</sup></b>	<b>Center # 2</b>	0	3.4E-05	0.520
	<b>Center # 3</b>	0	2.8E-05	0.614
<b>Fraction of all CD8+IFN<math>\gamma</math>+ out of all CD8<sup>+</sup></b>	<b>Center # 1</b>	2	-1.0E-03	0.581
	<b>Center # 2</b>	0	8.4E-04	0.683
	<b>Center # 3</b>	0.5	2.5E-04	0.647
<b>Fraction of all CD8+IL2<sup>+</sup> out of all CD8<sup>+</sup></b>	<b>Center # 1</b>	2	1.7E-05	0.537
	<b>Center # 2</b>	0	6.6E-05	0.549
	<b>Center # 3</b>	1	2.6E-05	0.588
<b>Fraction of all activated CD8<sup>+</sup></b>	<b>Center # 1</b>	2	-7.7E-04	0.591
	<b>Center # 2</b>	0	8.9E-04	0.690
	<b>Center # 3</b>	0.5	2.9E-04	0.634

## *Supplementary Section 2: Comparison of different immune response metrics*

For metrics of T cell response evaluated with ELISpot and flow cytometry and for IgG/IgM measures by Mindray assay, the Spearman correlation matrix was calculated as shown in Supplementary Figure S5.

### *NoS for M, N, and S protein correlations*

For all three pairwise comparisons of M, N, and S protein NoS, a high Spearman correlation coefficient was observed (M vs. N, 0.69; S vs. N, 0.69; S vs. M, 0.75; see also Supplementary Figure S5). NoS for the S protein was statistically significantly higher than NoS for the M and N proteins, and NoS for the M protein was higher than NoS for the N protein, although the values were very close (Wilcoxon paired test  $p$ -value  $< 1e-19$  for all comparisons). It is most likely that these results originate from the differences in sizes of these proteins, since the S protein is the largest among them, while the M and N protein sizes are comparable to one another and both are smaller than the S.

### *Flow Cytometry: CD4<sup>+</sup> and CD8<sup>+</sup> cell fraction correlations*

For all three pairwise comparisons of the fractions of CD4<sup>+</sup> cells expressing IFN $\gamma$  only, IL2 only, or both cytokines, statistically significant Spearman correlation coefficients were observed (IL2<sup>+</sup> vs. IFN $\gamma$ <sup>+</sup>, 0.41; IFN $\gamma$ <sup>+</sup> vs. IL2<sup>+</sup>IFN $\gamma$ <sup>+</sup>, 0.58; IL2<sup>+</sup> vs. IL2<sup>+</sup>IFN $\gamma$ <sup>+</sup>: 0.75; see also Supplementary Figure S5). The fraction of CD4<sup>+</sup> cells expressing IL2 only was significantly lower than the fraction of cells expressing IFN $\gamma$  only (Wilcoxon paired test  $p$ -value  $< 0.002$ ), and the fraction of cells expressing both cytokines was lower than either of fractions of cells expressing one cytokine only (Wilcoxon paired test  $p$ -value  $< 1e-100$ ).

Additionally, the fraction of CD4<sup>+</sup> cells expressing IFN $\gamma$  only out of the total number of CD4<sup>+</sup> cells was compared with the fraction of CD8<sup>+</sup> cells expressing IFN $\gamma$  only out of the total number of CD8<sup>+</sup> cells, and a statistically significant Spearman correlation coefficient of 0.53 was observed. Similarly, the fraction of CD4<sup>+</sup> cells expressing IL2 only out of the total number of CD4<sup>+</sup> cells was correlated with the fraction of CD8<sup>+</sup> cells expressing IL2 only out of total number of CD8<sup>+</sup> cells, with a Spearman correlation coefficient of 0.47 (see also Supplementary Figure S5).



### Correlation between ELISpot and flow cytometry

In order to perform additional comparisons between ELISpot and flow cytometry, we computed the fraction of all CD4<sup>+</sup>/CD8<sup>+</sup> cells expressing IFN $\gamma$  (cells also expressing IL2 included) and summed NoS for M, N, and S. No correlation was observed between any ELISpot NoS and any fractions of CD8<sup>+</sup> cells. On the contrary, NoS for all proteins and their combination was significantly correlated with all CD4<sup>+</sup> cell fractions, with a Spearman correlation coefficient in a range from 0.38 to 0.56 for different comparison pairs (see also Supplementary Figure S5).

### Correlation between IgG antibody levels and T cell immune response metrics

A Spearman correlation of ~0.6 was observed between IgG and ELISpot NoS for each of three proteins. Compared with flow cytometry results, IgG antibody levels were most strongly correlated with the fraction of CD4<sup>+</sup> cells expressing both IFN $\gamma$  and IL2 out of the total number of CD4<sup>+</sup> cells (Spearman correlation coefficient 0.52), followed by those expressing the IL2-only fraction (Spearman correlation coefficient 0.45) and the IFN $\gamma$ -only fraction (Spearman correlation coefficient 0.34). None of the CD8<sup>+</sup> cell fractions demonstrated a high correlation with IgG antibody levels (see also Supplementary Figure S5).

We additionally studied whether the observed correlation is only a result of the existence of two main groups of patients, one with very low responses for both IgG and T cell immunity and another with high responses for both cases, or whether there is an intermediate group of patients with both an antibody response and an intermediate T cell response. In order to do that, we analyzed the distribution of S NoS and of the fraction of CD4<sup>+</sup> cells expressing both IFN $\gamma$  and IL2 out of the total number of CD4<sup>+</sup> cells as a function of IgG levels split by deciles, using ridgeline plots (Supplementary Figure S6). For the fraction of CD4<sup>+</sup> cells expressing both IFN $\gamma$  and IL2 out of the total number of CD4<sup>+</sup> cells, there is a smooth transition not only with average levels but also with the whole distribution moving towards higher values as IgG levels were increased (similar results were observed for all other CD4<sup>+</sup> cell fractions; not given in the paper). On the contrary, for S NoS there was no transition, but the density distribution for intermediate levels can be interpreted as a mixture of distributions observed for high and low IgG levels (similar results were observed for M and N NoS; not given in the paper). It should be noted that results provided for ELISpot NoS should be

viewed with some doubt, since the distribution of NoS is inherently not normal, and ridgeline plots employ kernel-density estimates using Gaussian kernels.

### *Supplementary Section 3: Kaplan-Meier Curves*

We observed all the individuals included in the study using the Moscow State COVID-19 Observation registry, which includes information about patient illness and vaccination. In order to perform an analysis using Kaplan-Meier curves, we excluded from the analysis individuals with pre-inclusion clinically confirmed COVID-19, as well as those who were included in the clinical trial of vaccine or who had been vaccinated before the inclusion. Next, we excluded all the patients who were added into the registry as ill within five days after inclusion in the study in order to exclude patients who might already have been ill at the moment of inclusion and blood collection. All the remaining participants were then considered as eligible for post-inclusion observation. Thus, by the end of observation at the beginning of April, 2021, among the 4,027 participants who were eligible for the post-inclusion observation, a total of 259 post-inclusion cases of COVID-19 were registered.

For these participants, we employed the Kaplan–Meier estimator. The date of the patient’s illness according to the Observation registry was considered to be the date of the ‘event’, while the date of vaccination or the date of last observation, whichever came first, was considered to be the right-censoring date. After that, the classical Kaplan-Meier estimator was used to study the survival function in different subgroups of patients.

*Supplementary Section 4: Correlation between different serological tests and virus-neutralizing activity*

Within the cohort we selected a group of individuals whose IgG titers, estimated using the automated analyzer (Mindray, China; here and below mentioned as ‘IgG (Mindray)’), were uniformly represented. Because of the limited sample volume, these individuals were additionally tested either for virus-neutralizing activity (VNA) and spike S-protein-specific IgG antibodies or for S- and nucleocapsid N-protein specific IgGs.

We first analyzed relations between S-protein-specific antibodies, N-protein-specific antibodies, and IgG (Mindray). We detected a strong correlation between S- and N-protein-specific antibodies. We manually split all the individuals into four groups: a negative group, a group with correlated response, and groups with either only S-protein or only N-protein-specific antibodies (Supplementary Figure S10, panel A). The vast majority of the individuals with some response demonstrated antibodies against both S- and N-protein (76.5%), while S- and N-protein single-positive individuals represented only 8.4 and 15.1%, respectively. These data are in good agreement with the results of the ELISpot shown in Figure 3C.

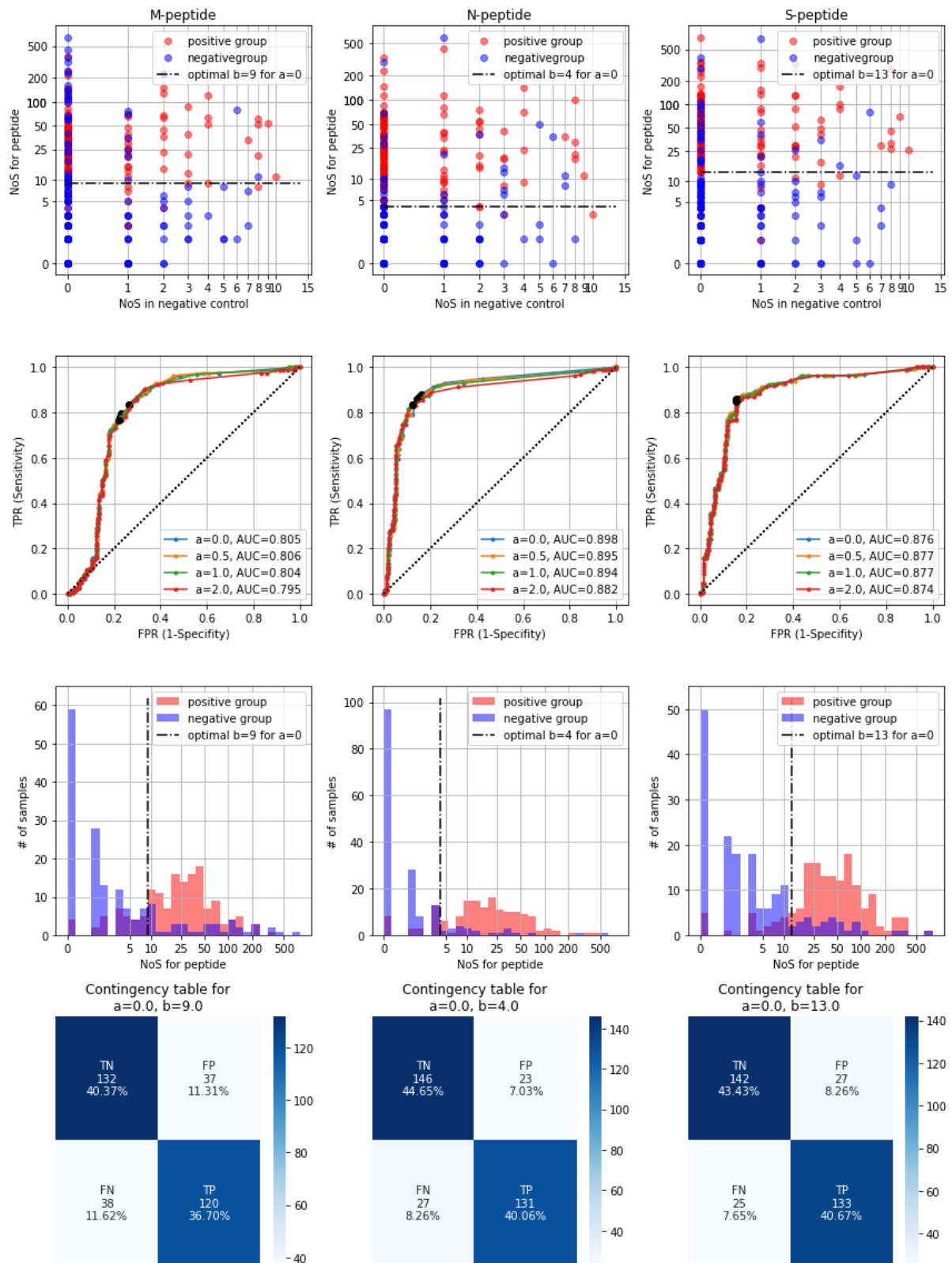
We also found a strong correlation between automated analyzer IgG (Mindray) titers and both S-protein and N-protein-specific antibodies. These results are in accordance with the manufacturer’s description, since this serological test was developed to detect antibodies specific to the full length of SARS-CoV-2 N protein and receptor binding domain (RBD) portion of the spike SARS-CoV-2 protein (Supplementary Figure S10, panel A).

We additionally analyzed the connections between VNA, S-protein-specific antibodies, and IgG (Mindray). We showed that VNA correlated with both IgG (Mindray) titer and S-protein-specific antibody levels (Supplementary Figure S10, panel B). The highest VNA was detected in individuals with high IgG (Mindray) titer and high S-protein-specific antibody levels, making up the Q4 and Q5 quantiles of IgG (Mindray) (see Figure 5A and the corresponding section of the main text for description of quantiles). Particularly, we found a significant virus-neutralizing activity among individuals making up the Q3 quantile (with IgG (Mindray) values in a range 0.97–8.33 AU/mL). This finding probably explains the protection against SARS-CoV-2 infection observed for this quantile. However, there was no difference in VNA between Q1 and Q2 quantiles. It is still possible that Q2 possesses VNA that are lower than the minimal plasma dilution used in our study, and protectivity found for

Q2 may be also explained by the presence of VNA in this group. Still, in this case VNA would be significantly lower in the Q2 quantile than in Q3.

# Supplementary Figures

Figure S1



**Supplementary Figure S1.** Selection of optimal positivity criteria for ELISpot based on patient groups.

**Left column** shows results for M-protein; **middle**, for N-protein; **right**, for S-protein.

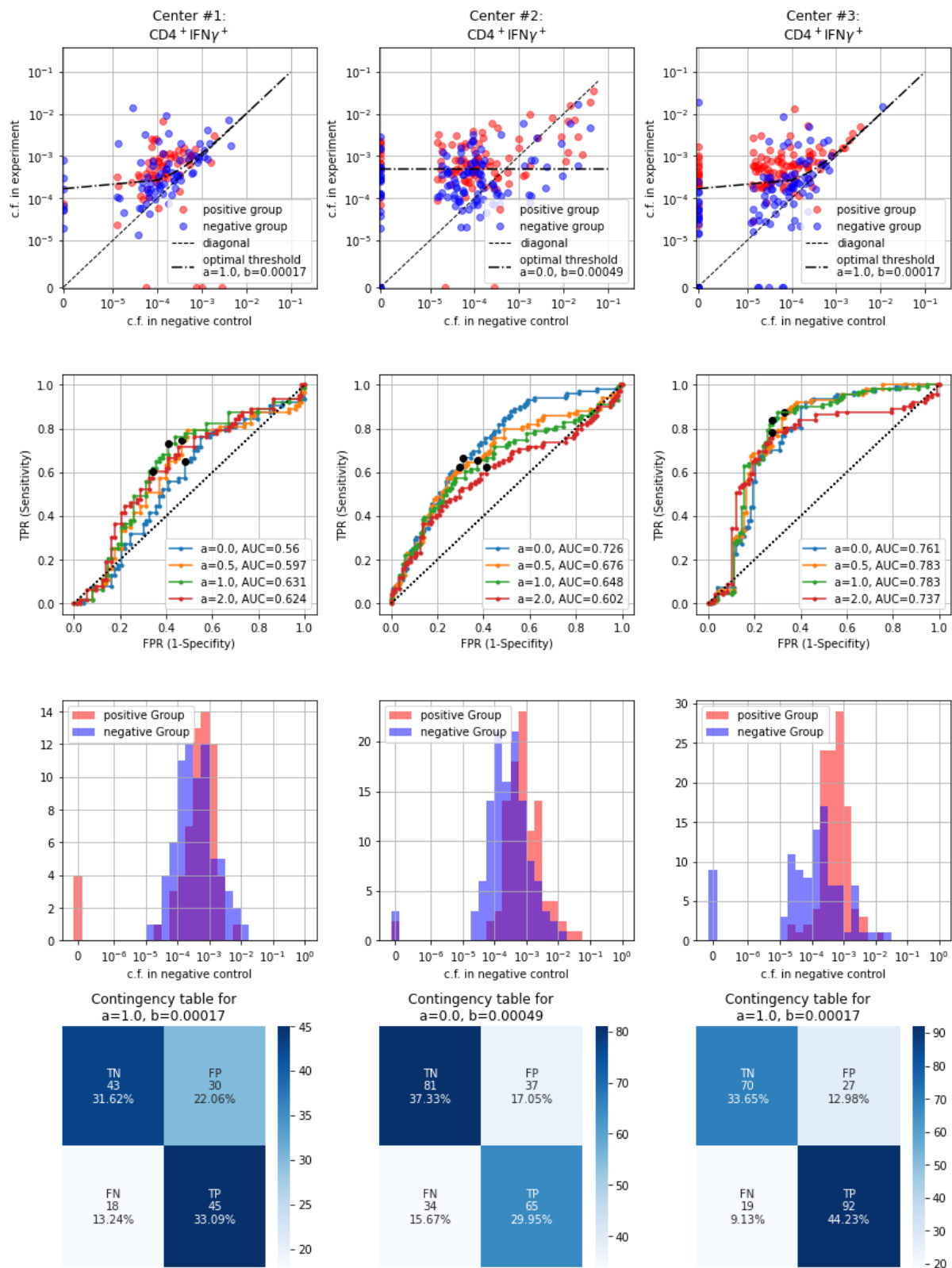
**Top row:** scatter plots for connection between negative control and stimulated sample; one dot corresponds to one patient. Red dots are used to show patients from the positive group; blue dots are used to show patients from the negative group. The dotted black line shows optimal separation criteria selecting based on ROC curve analysis with  $a=0$ .

**Second row from the top:** ROC curves for linear separation rule  $\text{NoS}_{\{\text{protein}\}} > a \cdot \text{NoS}_{\{\text{negative\_control}\}} + b$  with 'a' out of  $\{0;0.5;1;2\}$  and variable 'b'. Black dots show the optimal point for each ROC curve (defined as the point of the curve closest to  $\text{FPR}=0$ ,  $\text{TPR}=1$ ).

**Third row from top:** histograms showing distribution of NoS in experiment in positive group and negative group.

**Bottom row:** contingency table for optimal rule selected on the basis of ROC curves for  $a=0$  with 'b' above the table. 'TN' stands for 'True Negative', 'TP' for 'True Positive', 'FN' for 'False Negative', 'FP' for 'False Positive', with positive and negative group labels treated as true labels '1' and '0', respectively, and optimal rule-based labels used as predicted labels.

Figure S2



**Supplementary Figure S2.** Selection of optimal positivity criteria for flow cytometry cell fractions based on patient groups.



**Left column** shows results for the fraction of  $CD4^+IFN\gamma^+$  cells out of all  $CD4^+$  cells in Center 1; **middle**, in Center 2; **right**, in Center 3.

**Top row:** scatter plots for connection between negative control and stimulated sample; one dot corresponds to one patient. Red dots are used to show patients from the positive group; blue dots are used to show patients from the negative group. The dotted black line shows optimal separation criteria selected on the basis of ROC curve analysis.

**Second row from the top:** ROC curves for linear separation rule  $Fraction_{\{experiment\}} > a * Fraction_{\{negative\_control\}} + b$  with 'a' out of {0;0.5;1;2} and variable 'b'. Black dots show the optimal point for each ROC curve (defined as the point of the curve closest to  $FPR=0, TPR=1$ ).

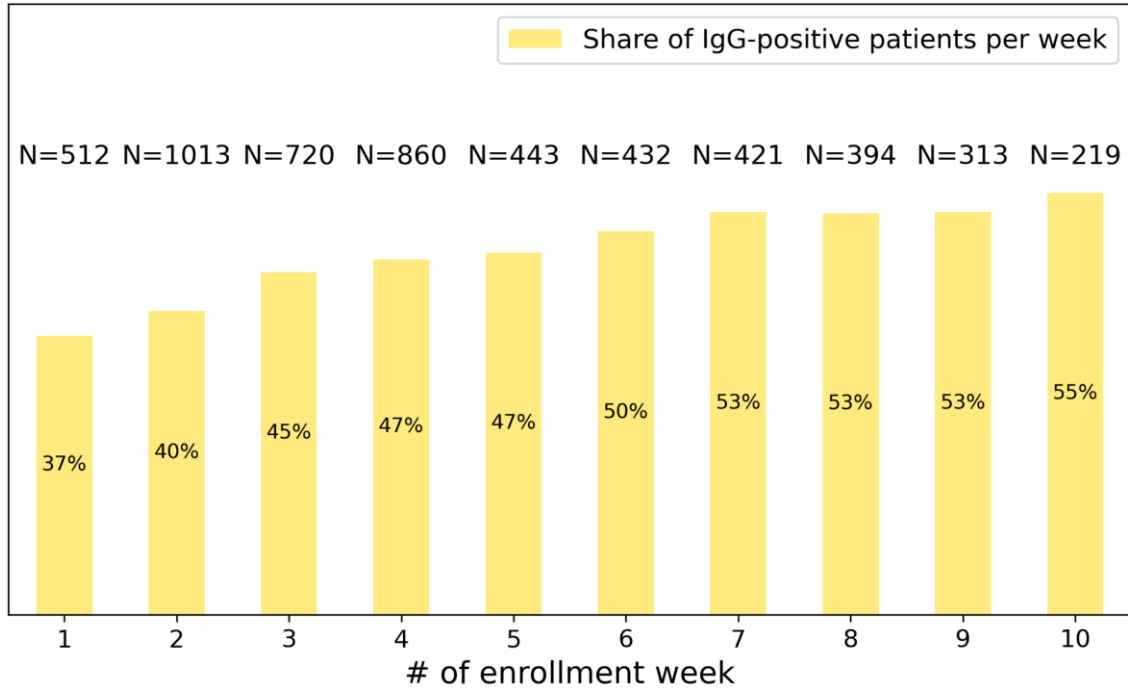
**Third row from top:** histograms showing distribution of cell fractions in experiment in positive group and negative group.

**Bottom row:** contingency tables for optimal rule selected based on ROC curves with 'a' and 'b' above the table. 'TN' stands for 'True Negative', 'TP' for 'True Positive', 'FN' for 'False Negative', 'FP' for 'False Positive', with positive and negative group labels treated as true labels '1' and '0', respectively, and optimal rule-based labels used as predicted labels.

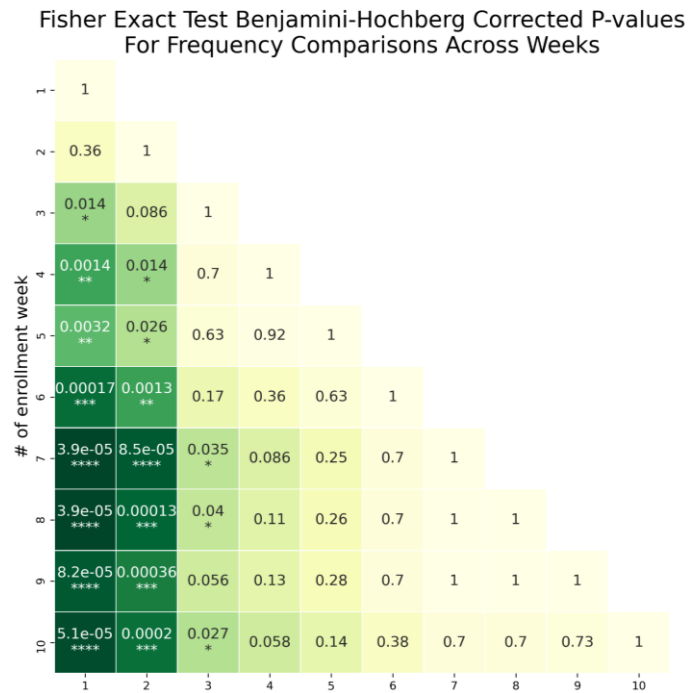
In all panels, 'c.f.' stands for 'cell fraction'

Figure S3

A



B

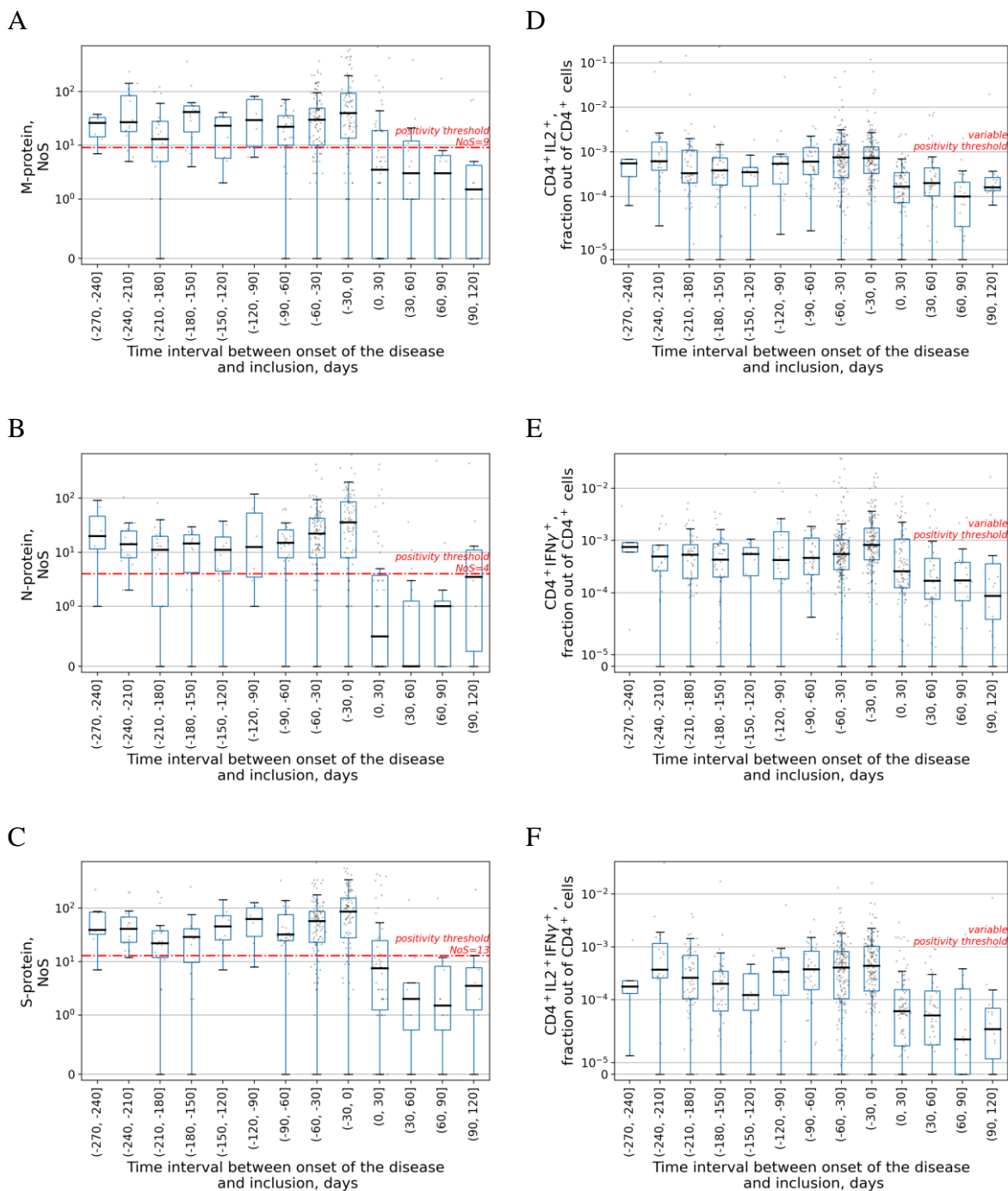


Supplementary Figure S3. Changes in share of IgG-positive patients per enrollment week

**(A):** Share of IgG-positive participants per enrollment week. Number of participants per week (N) is given above each bar.

**(B):** Benjamini-Hochberg corrected  $p$ -values for pairwise comparison of share of IgG-positive patients per week of inclusion.

Figure S4



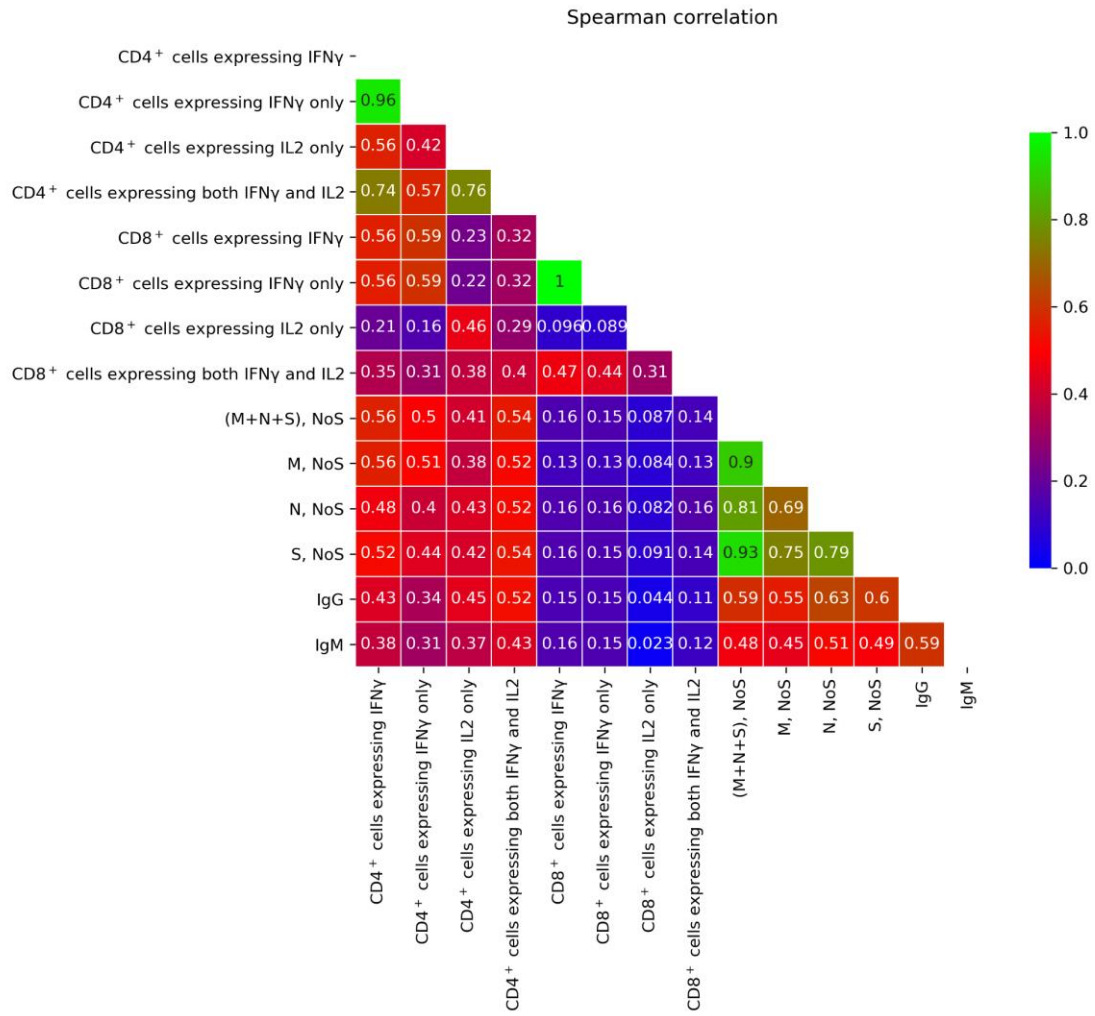
**Supplementary Figure S4.** Temporal stability of all ELISpot and flow cytometry

**(A),(B),(C):** Time dependence of the spots number for M, N, and S proteins in ELISpot assay, respectively. Each dot represents a single patient. Time is counted from the date of disease onset according to the official registry to the day of the inclusion in the study and thus serology testing. Time interval presented in each box-plot is 30 days. Red line represents a positivity threshold.

**(D),(E),(F):** Time dependence of the percentage of CD4<sup>+</sup> T cells expressing IL2, IFN $\gamma$ , or both cytokines, respectively, in flow cytometry assay. Each dot represents a single patient. Time is counted from the date of disease onset according to the official registry to the day of the inclusion in the study and thus serology testing. Time interval presented in each boxplot is 30 days. Positivity threshold was variable (see Supplementary Materials for more details) and thus not given here.

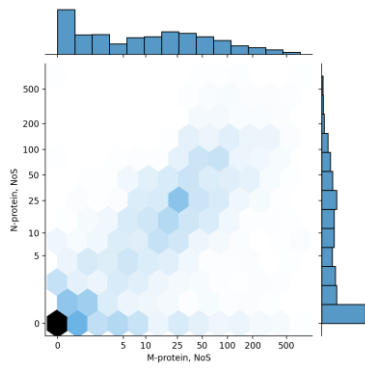
Figure S5

A

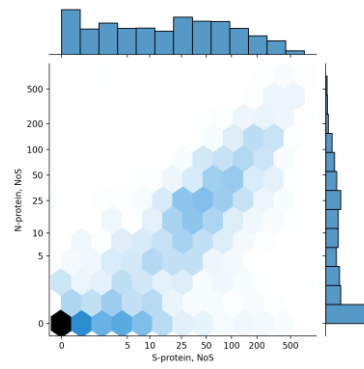


## ELISpot:

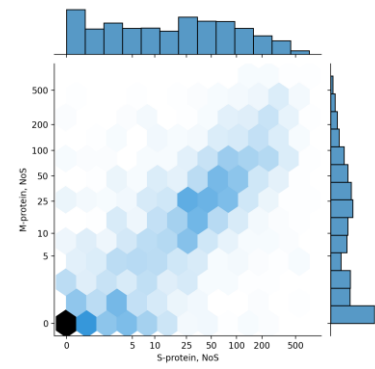
B



C

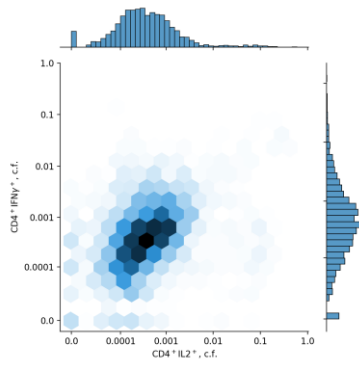


D

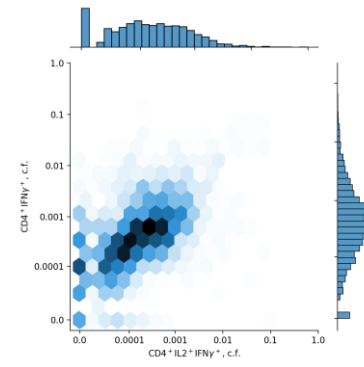


## Flow Cytometry CD4<sup>+</sup>:

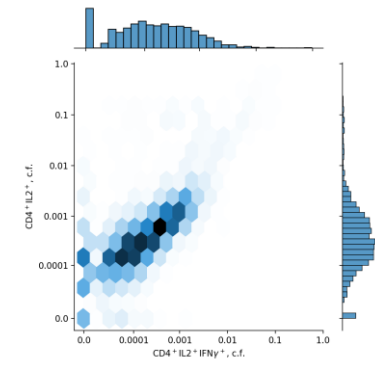
E



F

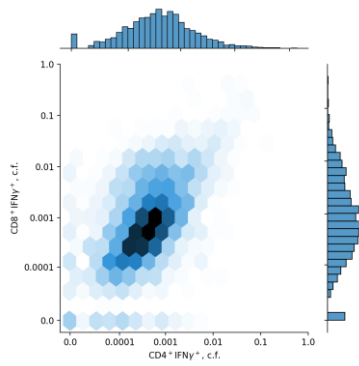


G

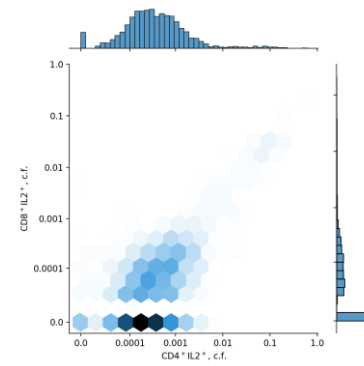


## Flow Cytometry CD4<sup>+</sup> vs CD8<sup>+</sup>:

H

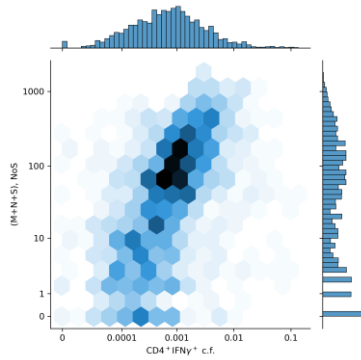


I



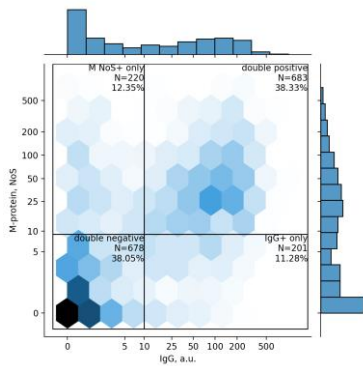
Flow Cytometry CD4<sup>+</sup> vs ELISpot:

J

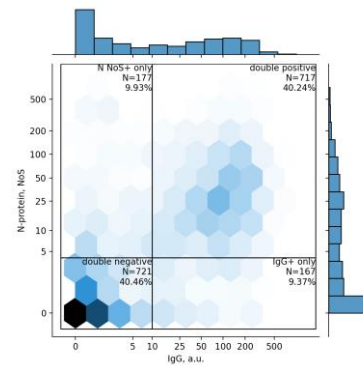


Antibodies and ELISpot:

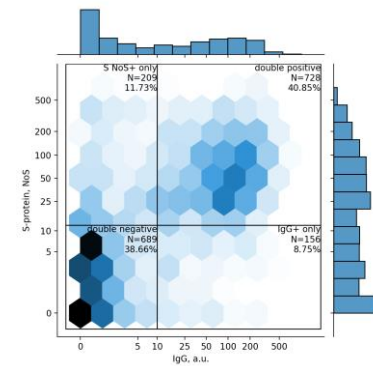
K



L

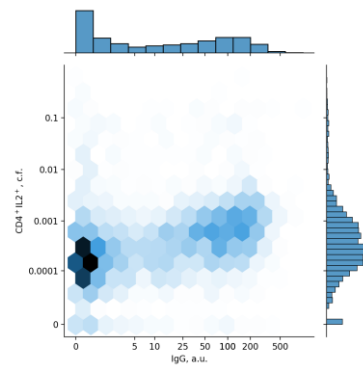


M

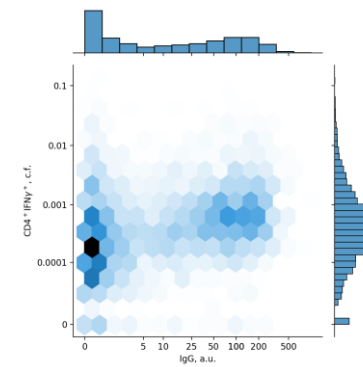


Antibodies and Flow Cytometry:

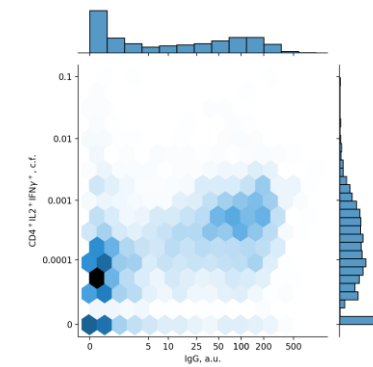
O



P



Q



Supplementary Figure S5. Comparison of different immune response metrics.



**(A)** Spearman correlation coefficient matrix for different metrics of immune response, with low correlation colored in blue, middle in red, and high in green (no negative correlations were observed)

**(B),(C),(D)** Density plots for pairwise comparison of NoS for different pairs of ELISpot proteins: M – S, S – N, and S – M, respectively. Each cell is colored according to the number of participants falling within this cell, with darker colors showing more participants. Histograms of value distribution are given along the corresponding axis.

**(E),(F),(G)** Density plots for pairwise comparison of activated CD4<sup>+</sup> cell fractions for different cytokines: IL2<sup>+</sup> – IFN $\gamma$ <sup>+</sup>, IL2<sup>+</sup>IFN $\gamma$ <sup>+</sup> – IFN $\gamma$ <sup>+</sup>, and IL2<sup>+</sup>IFN $\gamma$ <sup>+</sup> – IL2<sup>+</sup>, respectively. Each cell is colored according to the number of participants falling within this cell, with darker colors showing more participants. Histograms of value distribution are given along the corresponding axis; ‘c.f.’ stands for ‘cell fraction’.

**(H),(I)** Density plots for pairwise comparison of activated CD4<sup>+</sup> and CD8<sup>+</sup> cell fractions for different cytokines: CD4<sup>+</sup>IFN $\gamma$ <sup>+</sup> – CD8<sup>+</sup>IFN $\gamma$ <sup>+</sup> and CD4<sup>+</sup>IL2<sup>+</sup> – CD8<sup>+</sup>IFN $\gamma$ <sup>+</sup>, respectively. Each cell is colored according to the number of participants falling within this cell, with darker colors showing more participants. Histograms of value distribution are given along the corresponding axis; ‘c.f.’ stands for ‘cell fraction’.

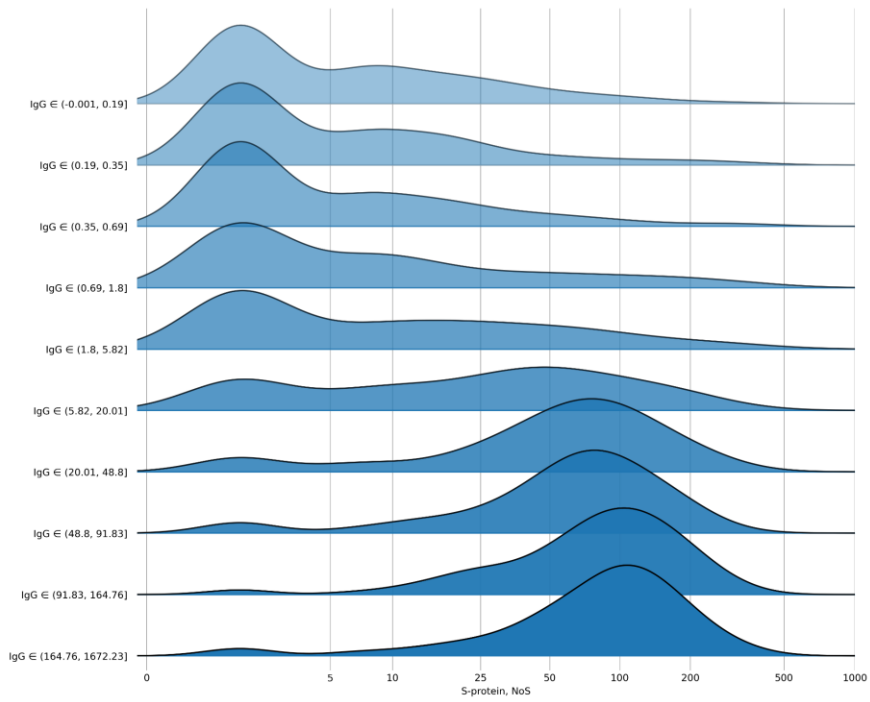
**(J)** Density plot for pairwise comparison of all activated CD4<sup>+</sup> cells expressing IFN $\gamma$  versus total number of spots for the M, N, and S proteins. Each cell is colored according to the number of participants falling within this cell, with darker colors showing more participants. Histograms of value distribution are given along the corresponding axis.

**(K),(L),(M)** Density plots for pairwise comparison of levels of IgG and of NoS for different pairs of ELISpot proteins: M, N, and S, respectively. Each cell is colored according to the number of participants falling within this cell, with darker colors showing more participants. Histograms of value distribution are given along the corresponding axis.

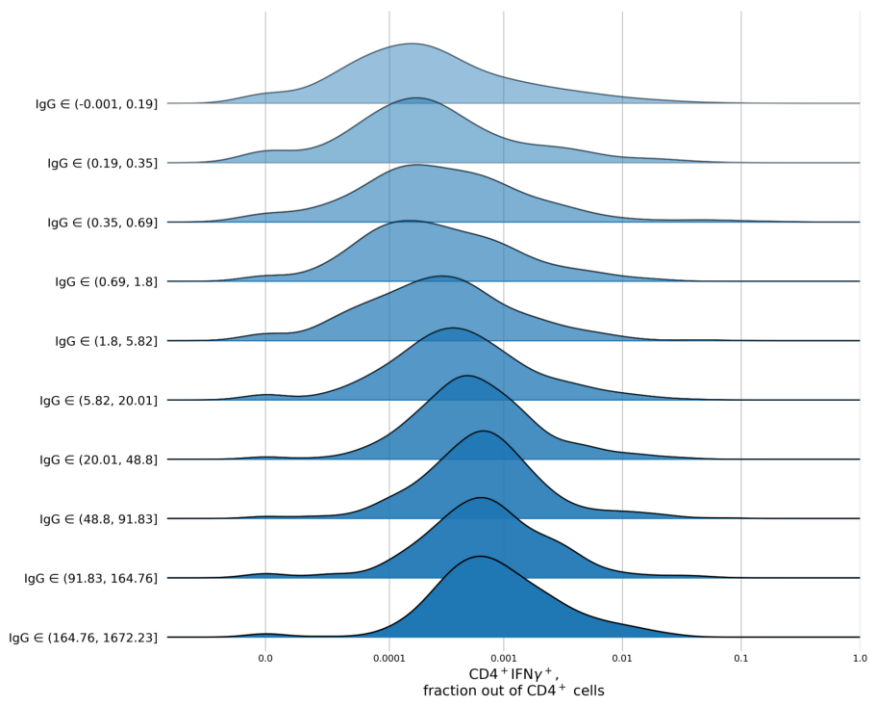
**(O),(P),(Q)** Density plots for pairwise comparison of levels of IgG and activated CD4<sup>+</sup> cells fractions for different cytokines: IL2<sup>+</sup>, IFN $\gamma$ <sup>+</sup>, and IL2<sup>+</sup>IFN $\gamma$ <sup>+</sup>, respectively. Each cell is colored according to the number of participants falling within this cell, with darker colors showing more participants. Histograms of value distribution are given along the corresponding axis; ‘c.f.’ stands for ‘cell fraction’.

Figure S6

A



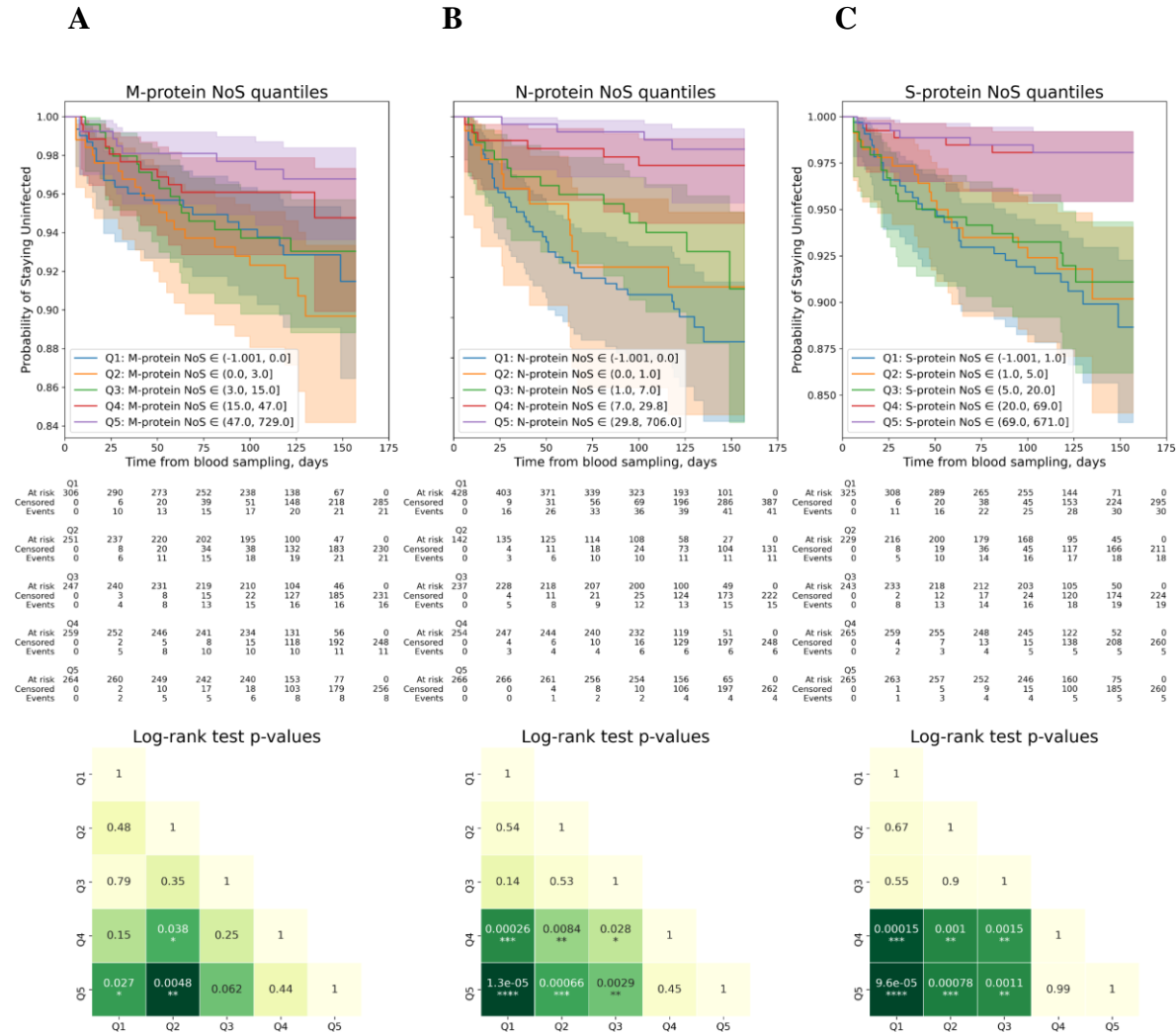
B

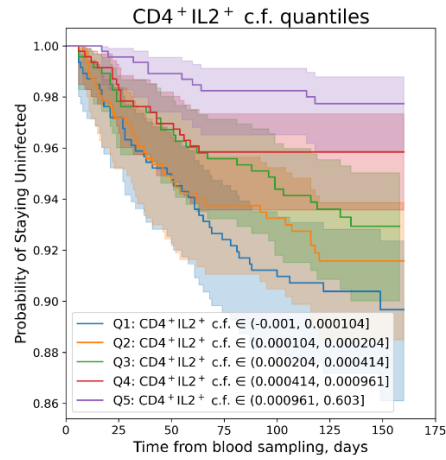


**Supplementary Figure S6.** Ridgeline plots for T cell immunity metrics as a function of antibody levels.

**(A), (B)** Distribution per decile of IgG of ELISpot S NoS and flow cytometry CD4<sup>+</sup> cells expressing IFN $\gamma$  out of the total number of CD4<sup>+</sup> cells, respectively. For patients from each IgG decile, the plot shows the kernel-density estimate for the corresponding T cell immunity metric obtained using the Gaussian kernel.

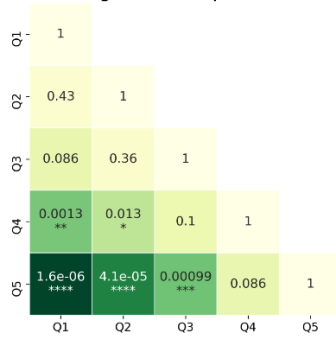
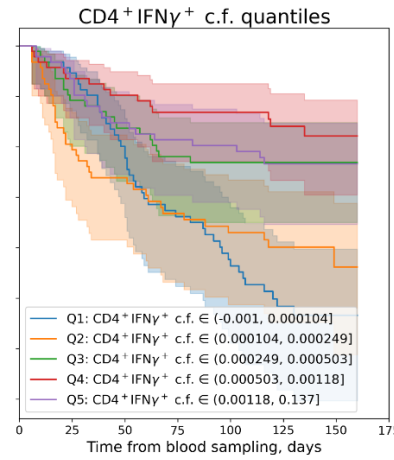
Figure S7



**D**

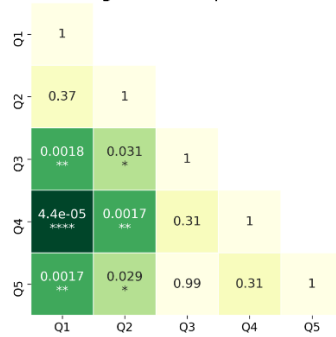
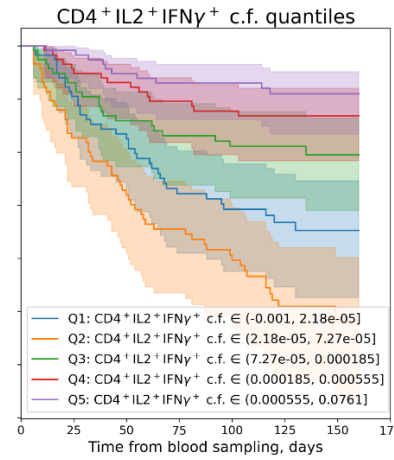
Q1	At risk	447	413	387	367	231	88	0
465	Censored	5	28	44	58	192	334	422
0	Events	13	24	34	40	42	43	43
Q2	At risk	444	412	382	370	261	101	0
465	Censored	8	29	55	65	168	328	429
0	Events	13	24	28	30	36	36	36
Q3	At risk	447	427	404	392	307	116	0
465	Censored	8	23	41	48	130	319	435
0	Events	10	15	20	25	28	30	30
Q4	At risk	454	438	422	414	322	86	0
465	Censored	3	13	24	32	124	360	446
0	Events	8	14	19	19	19	19	19
Q5	At risk	458	449	431	425	312	103	0
465	Censored	5	11	26	32	143	352	455
0	Events	2	5	8	8	10	10	10

Log-rank test p-values

**E**

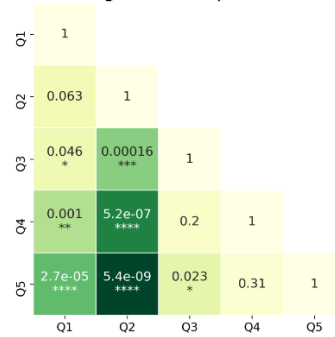
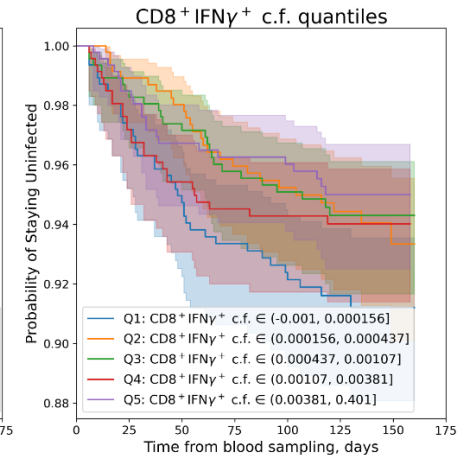
Q1	At risk	454	418	389	369	268	78	0
465	Censored	6	27	46	58	153	342	420
0	Events	5	20	30	38	44	45	45
Q2	At risk	437	410	376	360	263	85	0
465	Censored	9	31	59	72	167	344	429
0	Events	19	24	30	33	35	36	36
Q3	At risk	451	433	419	413	313	113	0
465	Censored	4	17	26	31	131	331	444
0	Events	10	15	20	21	21	21	21
Q4	At risk	455	442	423	411	309	111	0
465	Censored	4	14	30	42	142	339	450
0	Events	6	9	12	12	14	15	15
Q5	At risk	453	436	419	415	280	107	0
465	Censored	6	15	29	32	164	337	444
0	Events	6	14	17	18	21	21	21

Log-rank test p-values

**F**

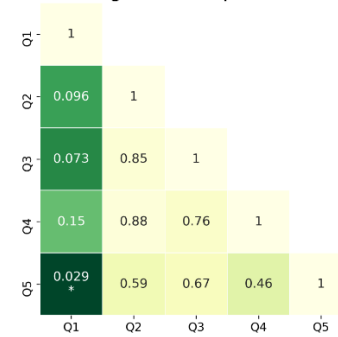
Q1	At risk	449	416	386	372	256	116	0
465	Censored	5	29	48	59	173	312	428
0	Events	11	20	31	34	36	37	37
Q2	At risk	438	409	378	363	257	96	0
465	Censored	7	24	48	57	155	315	429
0	Events	20	32	39	45	53	54	54
Q3	At risk	447	418	397	379	291	101	0
465	Censored	8	31	49	65	153	342	443
0	Events	8	16	19	21	22	22	22
Q4	At risk	458	449	428	421	316	99	0
465	Censored	1	8	25	30	134	351	450
0	Events	6	8	12	14	15	15	15
Q5	At risk	458	447	437	433	313	82	0
465	Censored	6	12	20	24	142	373	455
0	Events	1	6	8	8	10	10	10

Log-rank test p-values

**G**

Q1	At risk	446	416	391	376	245	75	0
465	Censored	6	25	44	54	183	352	427
0	Events	13	24	30	35	37	38	38
Q2	At risk	454	434	403	392	303	94	0
465	Censored	6	22	44	52	138	345	439
0	Events	5	9	18	21	24	26	26
Q3	At risk	451	432	416	401	317	132	0
465	Censored	6	20	30	42	123	308	440
0	Events	8	13	19	22	25	25	25
Q4	At risk	447	426	405	398	316	111	0
465	Censored	5	18	35	41	122	327	438
0	Events	13	21	25	26	27	27	27
Q5	At risk	452	431	411	401	252	82	0
465	Censored	6	19	37	46	191	361	443
0	Events	7	15	17	18	22	22	22

Log-rank test p-values



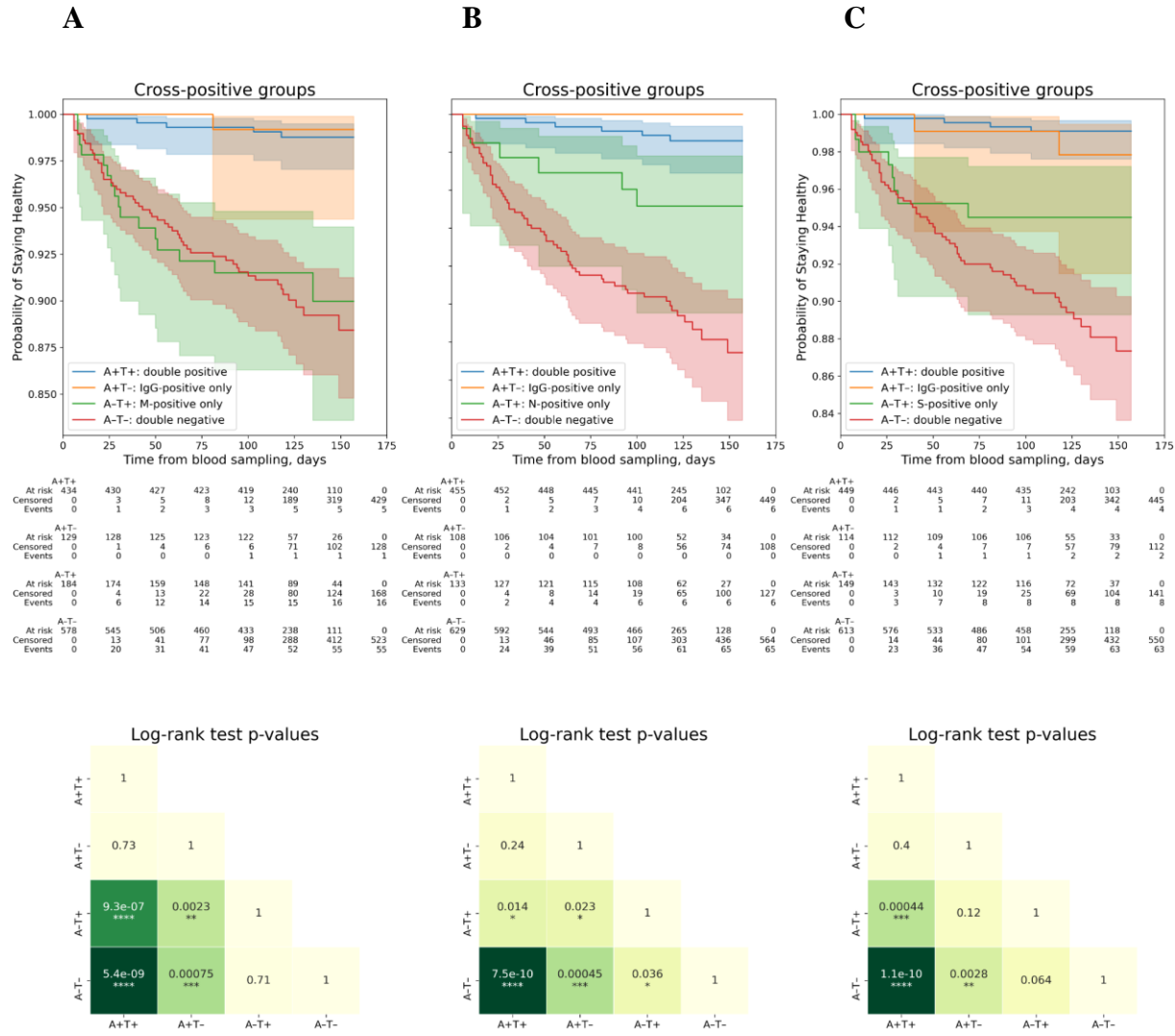
**Supplementary Figure S7.** Evaluation of effects of T cell immunity on COVID-19 infection rates.

**(A),(B),(C) Top:** Kaplan-Meyer curves for patients with different NoS for the M, N, and S proteins in ELISpot, respectively. The patients were split into five nearly equal groups by quantiles of NoS from Q1 to Q5, and a Kaplan-Meyer curve was built for each group (see Supplementary Materials for more details on Kaplan Meyer curves analysis). **Bottom:** log-rank test  $p$ -values for pairwise comparison of all five groups selected by quantiles.

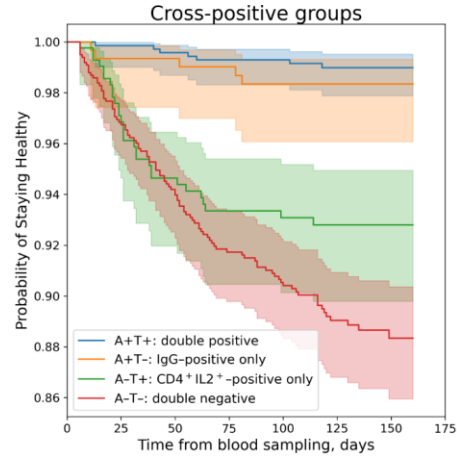
**(D),(E),(F) Top:** Kaplan-Meyer curves for patients with different  $CD4^+IL2^+$ ,  $CD4^+IFN\gamma^+$ , and  $CD4^+IL2^+IFN\gamma^+$  cell fractions out of all  $CD4^+$  cells, respectively. The patients were split into five nearly equal groups by quantiles of cell fraction from Q1 to Q5, and a Kaplan-Meyer curve was built for each group (see Supplementary Materials for more details on Kaplan Meyer curves analysis); ‘c.f.’ stands for ‘cell fraction’. **Bottom:** log-rank test  $p$ -values for pairwise comparison of all five groups selected by quantiles.

**(G) Top:** Kaplan-Meyer curves for patients with different  $CD8^+IFN\gamma^+$  cell fractions out of all  $CD8^+$  cells. All the patients were split into five nearly equal groups by quantiles of cell fraction from Q1 to Q5, and a Kaplan-Meyer curve was built for each group (see Supplementary Materials for more details on Kaplan Meyer curves analysis); ‘c.f.’ stands for ‘cell fraction’. **Bottom:** log-rank test  $p$ -values for pairwise comparison of all 5 groups selected by quantiles.

Figure S8

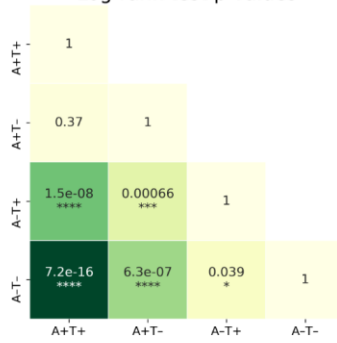


**D**

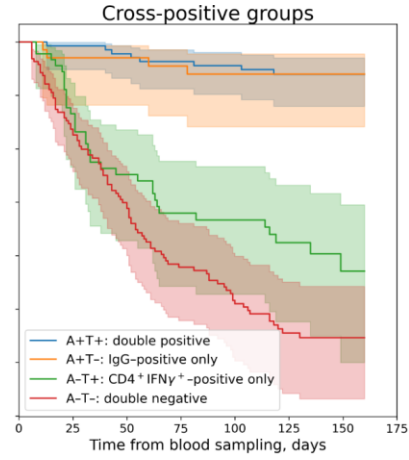


A+T+	708	701	695	690	506	152	0
At risk	711	701	695	690	506	152	0
Censored	0	2	7	11	16	198	552
Events	0	1	3	5	7	7	704
A+T-	303	299	294	290	208	93	0
At risk	308	299	294	290	208	93	0
Censored	0	3	7	11	13	95	210
Events	0	2	2	3	5	5	303
A-T+	418	397	375	347	339	271	91
At risk	418	397	375	347	339	271	91
Censored	0	8	21	44	51	118	298
Events	0	13	22	27	28	29	29
A-T-	989	860	783	739	531	219	0
At risk	989	860	783	739	531	219	0
Censored	0	16	71	128	161	359	668
Events	0	32	58	78	89	99	102

Log-rank test p-values

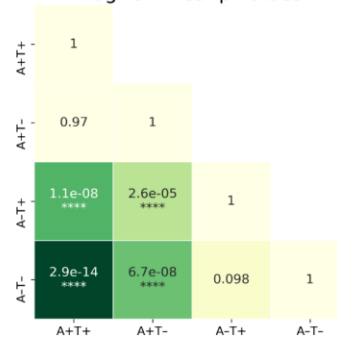


**E**

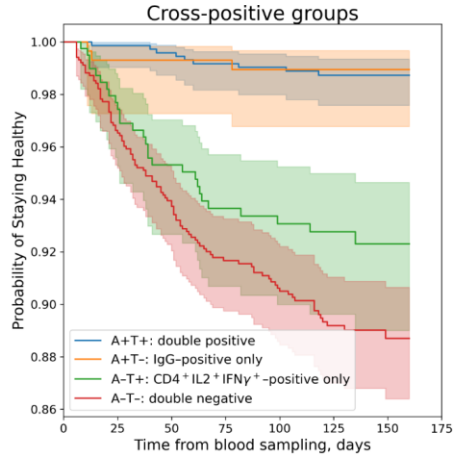


A+T+	680	673	665	659	466	142	0
At risk	684	673	665	659	466	142	0
Censored	0	3	8	14	19	210	534
Events	0	1	3	5	6	8	676
A+T-	331	327	324	321	248	103	0
At risk	335	327	324	321	248	103	0
Censored	0	2	6	8	10	83	228
Events	0	2	2	3	4	4	331
A-T+	453	431	406	375	361	262	115
At risk	453	431	406	375	361	262	115
Censored	0	10	25	50	63	159	304
Events	0	12	22	28	29	32	34
A-T-	954	907	829	755	717	540	195
At risk	954	907	829	755	717	540	195
Censored	0	14	67	122	149	318	662
Events	0	33	58	77	88	96	97

Log-rank test p-values

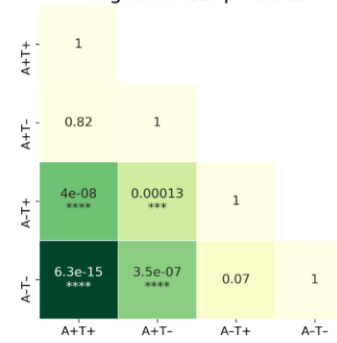


**F**



A+T+	727	720	713	708	511	145	0
At risk	730	720	713	708	511	145	0
Censored	0	2	7	11	15	210	576
Events	0	1	3	6	7	9	721
A+T-	284	280	276	272	203	100	0
At risk	289	280	276	272	203	100	0
Censored	0	3	7	11	14	83	186
Events	0	2	2	2	3	3	284
A-T+	392	373	355	325	314	247	90
At risk	392	373	355	325	314	247	90
Censored	0	9	19	43	52	118	274
Events	0	10	18	24	26	27	28
A-T-	1015	965	880	805	764	555	220
At risk	1015	965	880	805	764	555	220
Censored	0	15	73	129	160	359	692
Events	0	35	62	81	91	101	103

Log-rank test p-values





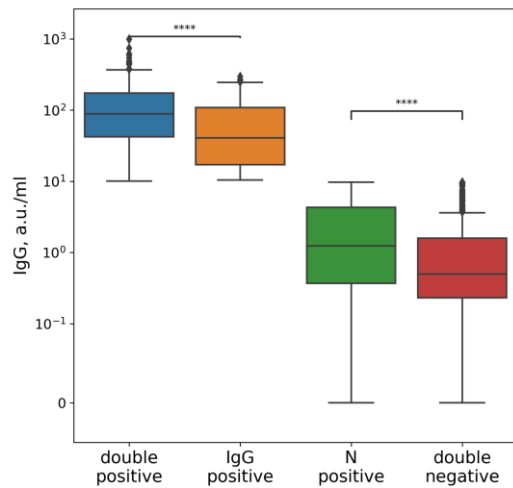
**Supplementary Figure S8.** Evaluation of connection between effects of antibody immunity and T cell immunity on COVID-19 infection rates.

**(A),(B),(C) Left:** Kaplan-Meier curves for patients with different positivity by IgG levels and by NoS for the M, N, and S proteins, respectively. The participants were split into four groups: positive only by antibodies (A+T-), positive only by NoS (A-T+), double-positive (A+T+), and double-negative (A-T-), with the positivity criteria discussed above used for the evaluation, and a Kaplan-Meier curve was built for each group (see Supplementary Materials for more details on Kaplan Meyer curves analysis). **Right:** log-rank test *p*-values for pairwise comparison of all four groups selected by positivity.

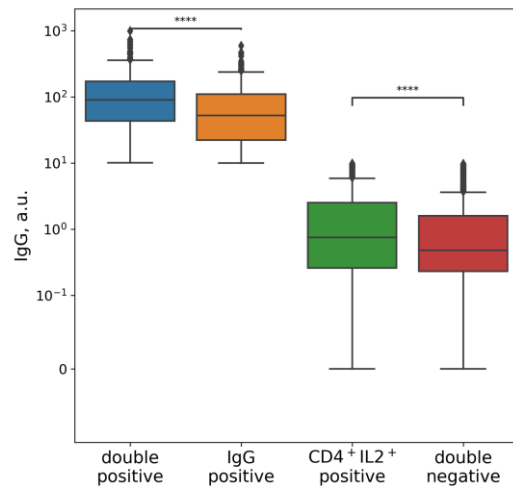
**(D),(E),(F) Left:** Kaplan-Meier curves for patients with different positivity by IgG levels and by CD4<sup>+</sup>IL2<sup>+</sup>, CD4<sup>+</sup>IFN $\gamma$ <sup>+</sup>, and CD4<sup>+</sup>IL2<sup>+</sup>IFN $\gamma$ <sup>+</sup> cell fractions out of all CD4<sup>+</sup> cells, respectively. All the participants were split into four groups: positive only by antibodies (A+T-), positive only by cell fraction (A-T+), double-positive (A+T+), and double-negative (A-T-), with the positivity criteria discussed above used for the evaluation, and a Kaplan-Meier curve was built for each group (see Supplementary Materials for more details on Kaplan Meyer curves analysis). **Right:** log-rank test *p*-values for pairwise comparison of all four groups selected by positivity.

Figure S9

A



B



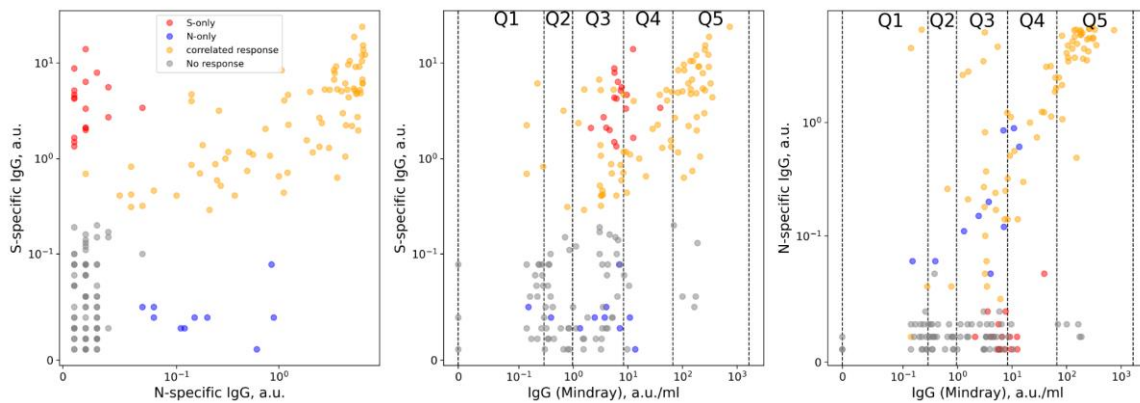
**Supplementary Figure S9.** Comparison of IgG levels in different positivity groups.

**(A)** IgG levels for patients with different positivity by IgG levels and by N-protein NoS in ELISpot. Comparison of groups with the same IgG positivity was performed by Mann-Whitney test and results are presented in the plot.

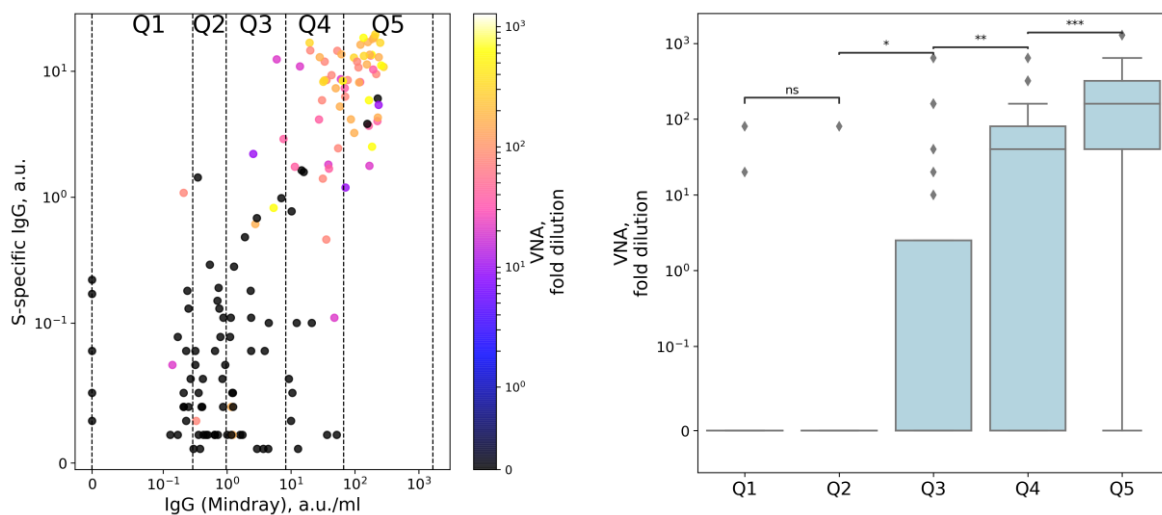
**(B)** IgG levels for patients with different positivity by IgG levels and by CD4<sup>+</sup>IL2<sup>+</sup> cell fractions out of all CD4<sup>+</sup> cells in flow cytometry. Comparison of groups with the same IgG positivity was performed by Mann-Whitney test, and results are presented in the plot.

Figure S10

A



B



**Supplementary Figure S10.** Correlation between different serological tests and virus-neutralizing activity.

(A) Comparisons of S-protein-specific antibodies with N-protein-specific antibodies (left), S-protein specific antibodies with IgG (Mindray) (middle), and N-protein-specific antibodies with IgG (Mindray) (right). All samples were manually splitted into four groups: a group with no response (shown in gray), a group with correlated response (shown in yellow), and groups with either only S-protein-specific or only N-protein-specific antibodies (shown in red and blue, respectively). In the middle and right panels, quantiles for IgG (Mindray) as used in Figure 5 are marked as vertical lines and labeled from Q1 to Q5.

**(B) Left:** Comparison of S-protein–specific antibodies with IgG (Mindray) colored with VNA measured in the same sample. Quantiles for IgG (Mindray) as used in Figure 5 are marked as vertical lines and labeled from Q1 to Q5. **Right:** Comparison of VNA in each quantile. Pairwise comparisons by Mann-Whitney test were performed for all neighboring pairs of quantiles.